resistance to radiation and induction of glutathione-regulating enzymes. Combined with other analyses, it could be possible that there are distinct groups of target genes regulated by mutant NRF2 in ESC cells. One group is sensitive to the amount of NRF2 and includes genes associated with cell proliferation, colony formation, and 5-FU resistance. The other is relatively resistant to NRF2 reduction and is responsible for attachment-independent survival and radiation resistance.

Our *in vitro* analyses also suggest that NRF2 activation could be associated with a poorer response to CRT in clinical cases of ESC. To examine this hypothesis, we carried out gene expression profiling, in view of the difficulty in collecting sufficient samples of pre-CRT tumors for mutation analysis. A number of previous studies have reported the identification of biomarkers that are predictive of the response of ESC to 5-FU or 5-FU–based neoadjuvant CRT [32–34]. Previously reported molecular makers have been categorized into several groups, including those related to 5-FU metabolism (e.g., thymidylate synthase and thymidine phosphorylase), the DNA repair pathway (e.g., excision repair cross-complementing rodent repair deficiency, complementation group 1 [ERCC1] and TP53), hypoxia (hypoxia-inducible factor 1α and vascular endothelial growth factor), and apoptosis/survival signaling (e.g., survivin, Bax, epidermal growth factor receptor, and Cox2) [32]. We tested the association between the expression level of ERCC1 or survivin and the clinical response to CRT in our cohort, but found no significant relationship (ERCC1, $P = .209$; survivin, $P = .327$). In contrast to these studies focusing on molecules with functional associations, only a few studies have explored microarray data in an unbiased way to search for biomarkers predictive of CRT efficacy, and only a limited number of cases ($n = 13$, 19, or 20) were examined [35–37].

In the present study, we adopted a different approach because NRF2 regulates a network of genes related to various molecular pathways at a different dose-response interaction. Instead of focusing on the expression of individual genes, we carried out "pathway analysis," which seems to be more relevant to biologic phenotypes, including therapeutic response [38]. Based on the gene expression data for ESC cell lines, we extracted a number of functionally annotated pathways whose expression was associated with the presence of *NRF2* mutation, which was also supported by ChIP-seq data of NRF2. We then used microarray data for the largest pre-CTR biopsy cohort ever reported (33 cases) and evaluated these pathways for predictive and prognostic utility. In total, up-regulation of 15 pathways was found to be significantly associated with a poor response to CRT and unfavorable prognosis, and our analysis revealed that expression of the gene sets related to oxidative stress and the immune response is associated with the clinical response of ESC to CRT and patient prognosis.

References

[1] Ferlay J, Shin HR, Bray F, Forman D, Mathers C, and Parkin DM (2010). Estimates of worldwide burden of cancer in 2008. *Int J Cancer* **127**, 2893–2917.

[2] Parkin DM, Bray F, Ferlay J, and Pisani P (2005). Global cancer statistics, 2002. *CA Cancer J Clin* **55**, 74–108.

[3] Morita M, Kumashiro R, Kubo N, Nakashima Y, Yoshida R, Yoshinaga K, Saeki H, Emi Y, Kakeji Y, Sakaguchi Y, et al. (2010). Alcohol drinking, cigarette smoking, and the development of squamous cell carcinoma of the esophagus: epidemiology, clinical findings, and prevention. *Int J Clin Oncol* **15**, 126–134.

[4] Falk GW (2009). Risk factors for esophageal cancer development. *Surg Oncol Clin N Am* **18**, 469–485.

[5] Hamilton SR and Aaltonen LA (2000). *Pathology and Genetics of Tumors of the Digestive Systems. World Health Organization Classification of Tumours.* IARC Press, Lyon, France.

[6] Kleinberg L and Forastiere AA (2007). Chemoradiation in the management of esophageal cancer. *J Clin Oncol* **25**, 4110–4117.

[7] Chirieac LR, Swisher SG, Ajani JA, Komaki RR, Correa AM, Morris JS, Roth JA, Rashid A, Hamilton SR, and Wu TT (2005). Posttherapy pathologic stage predicts survival in patients with esophageal carcinoma receiving preoperative chemoradiation. *Cancer* **103**, 1347–1355.

[8] Berger AC, Farma J, Scott WJ, Freedman G, Weiner L, Cheng JD, Wang H, and Goldberg M (2005). Complete response to neoadjuvant chemoradiotherapy in esophageal carcinoma is associated with significantly improved survival. *J Clin Oncol* **23**, 4330–4337.

[9] Martin RC, Liu Q, Wo JM, Ray MB, and Li Y (2007). Chemoprevention of carcinogenic progression to esophageal adenocarcinoma by the manganese superoxide dismutase supplementation. *Clin Cancer Res* **13**, 5176–5182.

[10] Cao L, Xu X, Cao LL, Wang RH, Coumoul X, Kim SS, and Deng CX (2007). Absence of full-length Brca1 sensitizes mice to oxidative stress and carcinogen-induced tumorigenesis in the esophagus and forestomach. *Carcinogenesis* **28**, 1401–1407.

[11] Chen X, Ding YW, Yang G, Bondoc F, Lee MJ, and Yang CS (2000). Oxidative damage in an esophageal adenocarcinoma model with rats. *Carcinogenesis* **21**, 257–263.

[12] Motohashi H and Yamamoto M (2004). Nrf2-Keap1 defines a physiologically important stress response mechanism. *Trends Mol Med* **10**, 549–557.

[13] Tong KI, Kobayashi A, Katsuoka F, and Yamamoto M (2006). Two-site substrate recognition model for the Keap1-Nrf2 system: a hinge and latch mechanism. *Biol Chem* **387**, 1311–1320.

[14] Ohta T, Iijima K, Miyamoto M, Nakahara I, Tanaka H, Ohtsuji M, Suzuki T, Kobayashi A, Yokota J, Sakiyama T, et al. (2008). Loss of Keap1 function activates Nrf2 and provides advantages for lung cancer cell growth. *Cancer Res* **68**, 1303–1309.

[15] Shibata T, Kokubu A, Gotoh M, Ojima H, Ohta T, Yamamoto M, and Hirohashi S (2008). Genetic alteration of Keap1 confers constitutive Nrf2 activation and resistance to chemotherapy in gallbladder cancer. *Gastroenterology* **135**, 1358–1368.

[16] Lee DF, Kuo HP, Liu M, Chou CK, Xia W, Du Y, Shen J, Chen CT, Huo L, Hsu MC, et al. (2009). KEAP1 E3 ligase-mediated downregulation of NF-κB signaling by targeting IKKβ. *Mol Cell* **36**, 131–140.

[17] Takahashi T, Sonobe M, Menju T, Nakayama E, Mino N, Iwakiri S, Nagai S, Sato K, Miyahara R, Okubo K, et al. (2010). Mutations in Keap1 are a potential prognostic factor in resected non–small cell lung cancer. *J Surg Oncol* **101**, 500–506.

[18] Zhang P, Singh A, Yegnasubramanian S, Esopi D, Kombairaju P, Bodas M, Wu H, Bova SG, and Biswal S (2010). Loss of Kelch-like ECH-associated protein 1 function in prostate cancer cells causes chemoresistance and radioresistance and promotes tumor growth. *Mol Cancer Ther* **9**, 336–346.

[19] Shibata T, Ohta T, Tong KI, Kokubu A, Odogawa R, Tsuta K, Asamura H, Yamamoto M, and Hirohashi S (2008). Cancer related mutations in NRF2 impair its recognition by Keap1-Cul3 E3 ligase and promote malignancy. *Proc Natl Acad Sci USA* **105**, 13568–13573.

[20] Narisawa-Saito M, Handa K, Yugawa T, Ohno S, Fujita M, and Kiyono T (2007). HPV16 E6-mediated stabilization of ErbB2 in neoplastic transformation of human cervical keratinocytes. *Oncogene* **26**, 2988–2996.

[21] Malhotra D, Portales-Casamar E, Singh A, Srivastava S, Arenillas D, Happel C, Shyr C, Wakabayashi N, Kensler TW, Wasserman WW, et al. (2010). Global mapping of binding sites for Nrf2 identifies novel targets in cell survival response through ChIP-Seq profiling and network analysis. *Nucleic Acids Res* **38**, 5718–5734.

[22] Duchesne GM (1994). Fundamental bases of combined therapy in lung cancer: cell resistance to chemotherapy and radiotherapy. *Lung Cancer* **10**(suppl 1), S67–S72.

[23] Coleman CN, Bump EA, and Kramer RA (1988). Chemical modifiers of cancer treatment. *J Clin Oncol* **6**, 709–733.

[24] Harvey CJ, Thimmulappa RK, Singh A, Blake DJ, Ling G, Wakabayashi N, Fujii J, Myers A, and Biswal S (2009). Nrf2-regulated glutathione recycling independent of biosynthesis is critical for cell survival during oxidative stress. *Free Radic Biol Med* **46**, 443–453.

[25] Ashida A, Boku N, Aoyagi K, Sato H, Tsubosa Y, Minashi K, Muto M, Ohtsu A, Ochiai A, Yoshida T, et al. (2006). Expression profiling of esophageal squamous cell carcinoma patients treated with definitive chemoradiotherapy: clinical implications. *Int J Oncol* **28**, 1345–1352.

[26] Kim YR, Oh JE, Kim MS, Kang MR, Park SW, Han JY, Eom HS, Yoo NJ, and Lee SH (2010). Oncogenic NRF2 mutations in squamous cell carcinomas of oesophagus and skin. *J Pathol* **220**, 446–451.

[27] Morita S, Yano M, Tsujinaka T, Ogawa A, Taniguchi M, Kaneko K, Shiozaki H, Doki Y, Inoue M, and Monden M (1998). Association between genetic polymorphisms of glutathione *S*-transferase P1 and *N*-acetyltransferase 2 and susceptibility to squamous-cell carcinoma of the esophagus. *Int J Cancer* **79**, 517–520.

[28] Rossini A, Rapozo DC, Soares Lima SC, Guimarães DP, Ferreira MA, Teixeira R, Kruel CD, Barros SG, Andreollo NA, Acatauassú R, et al. (2007). Polymorphisms of GSTP1 and GSTT1, but not of CYP2A6, CYP2E1 or GSTM1, modify the risk for esophageal cancer in a western population. *Carcinogenesis* **28**, 2537–2542.

[29] Zhang J, Schulz WA, Li Y, Wang R, Zotz R, Wen D, Siegel D, Ross D, Gabbert HE, and Sarbia M (2003). Association of NAD(P)H: quinone oxido-reductase 1 (NQO1) C609T polymorphism with esophageal squamous cell carcinoma in a German Caucasian and a northern Chinese population. *Carcinogenesis* **24**, 905–909.

[30] Wakabayashi N, Itoh K, Wakabayashi J, Motohashi H, Noda S, Takahashi S, Imakado S, Kotsuji T, Otsuka F, Roop DR, et al. (2003). Keap1-null mutation leads to postnatal lethality due to constitutive Nrf2 activation. *Nat Genet* **35**, 238–245.

[31] Singh A, Bodas M, Wakabayashi N, Bunz F, and Biswal S (2010). Gain of Nrf2 function in non–small-cell lung cancer cells confers radioresistance. *Antioxid Redox Signal* **13**, 1627–1637.

[32] Fareed KR, Kaye P, Soomro IN, Ilyas M, Martin S, Parsons SL, and Madhusudan S (2009). Biomarkers of response to therapy in oesophago-gastric cancer. *Gut* **58**, 127–143.

[33] Höfler H, Langer R, Ott K, and Keller G (2006). Prediction of response to neoadjuvant chemotherapy in carcinomas of the upper gastrointestinal tract. *Adv Exp Med Biol* **587**, 115–120.

[34] Luthra R, Luthra MG, Izzo J, Wu TT, Lopez-Alvarez E, Malhotra U, Choi IS, Zhang L, and Ajani JA (2006). Biomarkers of response to preoperative chemoradiation in esophageal cancers. *Semin Oncol* **33**(6 suppl 11), S2–S5.

[35] Kihara C, Tsunoda T, Tanaka T, Yamana H, Furukawa Y, Ono K, Kitahara O, Zembutsu H, Yanagawa R, Hirata K, et al. (2001). Prediction of sensitivity of esophageal tumors to adjuvant chemotherapy by cDNA microarray analysis of gene-expression profiles. *Cancer Res* **61**, 6474–6479.

[36] Luthra R, Wu TT, Luthra MG, Izzo J, Lopez-Alvarez E, Zhang L, Bailey J, Lee JH, Bresalier R, Rashid A, et al. (2006). Gene expression profiling of localized esophageal carcinomas: association with pathologic response to pre-operative chemoradiation. *J Clin Oncol* **24**, 259–267.

[37] Maher SG, Gillham CM, Duggan SP, Smyth PC, Miller N, Muldoon C, O'Byrne KJ, Sheils OM, Hollywood D, and Reynolds JV (2009). Gene expres-sion analysis of diagnostic biopsies predicts pathological response to neoadjuvant chemoradiotherapy of esophageal cancer. *Ann Surg* **250**, 729–737.

[38] Murat A, Migliavacca E, Gorlia T, Lambiv WL, Shay T, Hamou MF, de Tribolet N, Regli L, Wick W, Kouwenhoven MC, et al. (2008). Stem cell–related "self-renewal" signature and high epidermal growth factor receptor expression associated with resistance to concomitant chemoradiotherapy in glioblastoma. *J Clin Oncol* **26**, 3015–3024.

Table W1. Primers and Antibodies Used in This Study.

Gene Name	Forward PCR Primer	Reverse PCR Primer	Roche Universal, No.
GCLC	ggatgatgctaatgagtctgacc	tctactctccatccaatgtctgag	25
GSR	aacaacatcccaactgtggtc	ccatatttatgaatggcttcatctt	83
GAPDH	ccaaccgcgagaagatga	ccagaggcgtacagggatag	64

Antibodies Used in This Study

Antigen	Vendor		Clone No.	Dilution for Immunoblot
NRF2	Santa Cruz	Polyclonal		×500
β-Actin	Sigma	Monoclonal	AC-15	×1000
Lamin B1	Santa Cruz	Polyclonal		×500

Table W2. Pathologic Diagnosis of the Analyzed Sarcoma Cases.

Case No.	Histology
028-L	Leiomyosarcoma
029-L	Leiomyosarcoma
032-L	Leiomyosarcoma
034-L	Leiomyosarcoma
035-L	Leiomyosarcoma
037-L	Leiomyosarcoma
038-L	Leiomyosarcoma
039-L	Leiomyosarcoma
040-L	Leiomyosarcoma
093-mL	Liposarcoma, myxoid
094-mL	Liposarcoma, myxoid
095-mL	Liposarcoma, myxoid
096-mL	Liposarcoma, myxoid
097-mL	Liposarcoma, myxoid
098-mL	Liposarcoma, myxoid
099-mL	Liposarcoma, myxoid
100-mL	Liposarcoma, myxoid
101-mL	Liposarcoma, myxoid
102-mL	Liposarcoma, myxoid
103-mL	Liposarcoma, myxoid
105-mL	Liposarcoma, myxoid
106-mL	Liposarcoma, myxoid
108-mL	Liposarcoma, myxoid
020-M	MPNST
022-M	MPNST
023-M	MPNST
024-M	MPNST
025-M	MPNST
026-M	MPNST
056-mM	Myxoid MFH
057-mM	Myxoid MFH
060-mM	Myxoid MFH
062-mM	Myxoid MFH
063-mM	Myxoid MFH
065-mM	Myxoid MFH
066-mM	Myxoid MFH
067-mM	Myxoid MFH
068-mM	Myxoid MFH
069-mM	Myxoid MFH
070-mM	Myxoid MFH
073-pM	Pleomorphic MFH
074-pM	Pleomorphic MFH
075-pM	Pleomorphic MFH
077-pM	Pleomorphic MFH
078-pM	Pleomorphic MFH
079-pM	Pleomorphic MFH

Table W2. (*continued*)

| Case No.	Histology
080-pM	Pleomorphic MFH
081-pM	Pleomorphic MFH
082-pM	Pleomorphic MFH
083-pM	Pleomorphic MFH
084-pM	Pleomorphic MFH
085-pM	Pleomorphic MFH
086-pM	Pleomorphic MFH
087-pM	Pleomorphic MFH
088-pM	Pleomorphic MFH
RMS-16	Rhabdomyosarcoma
RMS-17	Rhabdomyosarcoma
RMS-18	Rhabdomyosarcoma
043-S	Synovial sarcoma
044-S	Synovial sarcoma
045-S	Synovial sarcoma
046-S	Synovial sarcoma
049-S	Synovial sarcoma
051-S	Synovial sarcoma
052-S	Synovial sarcoma
054-S	Synovial sarcoma
055-S	Synovial sarcoma
SS1	Synovial sarcoma
SS11	Synovial sarcoma
SS12	Synovial sarcoma
SS13	Synovial sarcoma
SS14	Synovial sarcoma
SS2	Synovial sarcoma
SS3	Synovial sarcoma
SS4	Synovial sarcoma
SS5	Synovial sarcoma
SS6	Synovial sarcoma
SS7	Synovial sarcoma
SS8	Synovial sarcoma
SS9	Synovial sarcoma
OS-41	Osteosarcoma
OS-44	Osteosarcoma
OS-45	Osteosarcoma
OS-46	Osteosarcoma
OS-47	Osteosarcoma
OS-49	Osteosarcoma
ES-01	Epithelioid sarcoma
ES-02	Epithelioid sarcoma
ES-04	Epithelioid sarcoma
ES-05	Epithelioid sarcoma
ES-06	Epithelioid sarcoma
ES-10	Epithelioid sarcoma
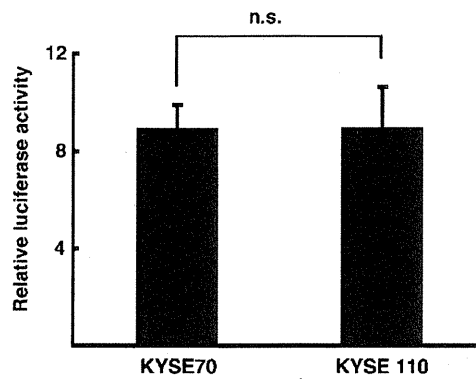
Figure W1. NRF2-dependent transcriptional activity in homozygous (KYSE70) and heterozygous (KYSE110) cells. n.s. indicates not significant.
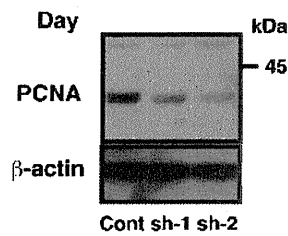

Figure W2. The expression of proliferating cell nuclear antigen (PCNA) in control (Cont) and *NRF2* (sh-1 and sh-2) shRNA expression clones. Protein extracted from each clone were immunoblotted with anti-PCNA mouse antibody (clone PC10; Cell Signaling Technologies, Danvers, MA). β-Actin was used as a loading control. Molecular marker is indicated on the right (kDa).
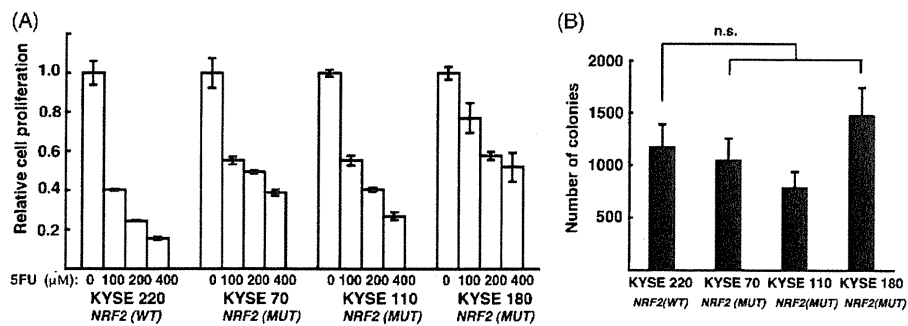
Figure W3. 5-FU sensitivity and basal colony formation capacity of *NRF2* wild-type (KYSE220) and mutated (KYSE70, KYSE110, KYSE180) ESC cell lines. (A) ESC cells were treated with various concentrations of 5-FU, and relative cell proliferation was shown. (B) Number of colony formation of each ESC cell was shown.
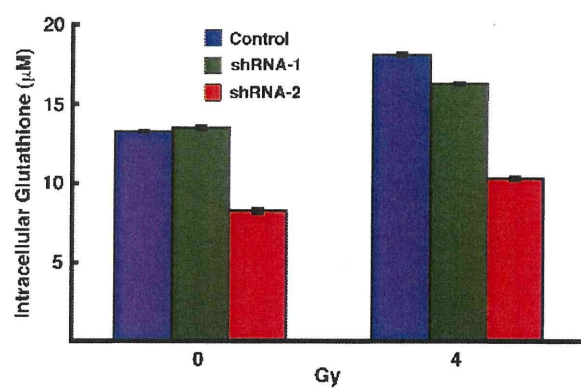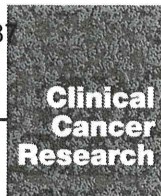
Figure W4. KYSE70 clones were irradiated (4 Gy), and the amount of intracellular reduced glutathione was measured after 24 hours.

Clinical
Cancer
Research

Cancer Therapy: Preclinical

Forkhead Transcription Factor FOXO1 is a Direct Target of Progestin to Inhibit Endometrial Epithelial Cell Growth

Satoru Kyo[1], Junko Sakaguchi[1], Tohru Kiyono[2], Yutaka Shimizu[3], Yoshiko Maida[1], Yasunari Mizumoto[1], Noriko Mori[1], Mitsuhiro Nakamura[1], Masahiro Takakura[1], Kiyohiko Miyake[2], Masaru Sakamoto[4], and Masaki Inoue[1]

Abstract

Purpose and experimental design: Despite the therapeutic utility of progestin in invasive and preinvasive endometrial neoplasias, the molecular mechanisms through which it exerts inhibitory effects on endometrial epithelial growth are largely unknown. The aim of the study was to clarify the molecular mechanisms of progestin action to endometrial epithelial cells using originally established *in vitro* and *in vivo* treatment models for immortalized and transformed endometrial epithelial cell lines that express progesterone receptor.

Results: In this model, progestin effectively inhibited the cell growth, inducing G0/G1 arrest rather than apoptosis without p21/WAF-1 induction. Using DNA microarray analysis, we identified 24 genes whose expression increased more than 10-fold on progestin treatment. Of these genes, we paid special attention to forkhead box transcription factor *FOXO1*, known as a key gene for endometrial decidualization. Progestin markedly induced *FOXO1* gene expression mainly in the nuclei *in vitro* and *in vivo*. This induction was not due to the canonical activation of FOXO1 via protein dephosphorylation but due to *FOXO1* promoter activation and mRNA induction. siRNA inhibition of *FOXO1* significantly attenuated the effects of progestin to inhibit endometrial epithelial cell growth. Disrupting Akt activity by the introduction of the dominant negative form of *Akt* increased nuclear FOXO1 accumulation and enhanced the effect of progestin.

Conclusion: These findings suggest that *FOXO1* is a direct target of progestin, implicating novel molecular mechanisms of progestin to eradicate endometrial neoplasia. *Clin Cancer Res; 17(3); 525–37. ©2010 AACR.*

Introduction

Endometrial cancer accounts for approximately 50,000 annual deaths worldwide and is the most common invasive neoplasia of the female genital tract in North America, where the incidence is highest (22.0 per 100,000 people per year) (1). The prognosis of this type of cancer is relatively favorable, mainly because the disease is usually diagnosed while it is limited to the corpus of the uterus, in which case the lesions are surgically treated by hysterectomy and bilateral salphingo-oophorectomy with or without retro-

peritoneal lymphadenectomy. However, patients with disseminated disease or those who have recurrence at distant sites after initial surgery have few options for systemic therapy. Because low-grade endometrial cancer is susceptible to hormonal influences in a significant proportion of progesterone receptor (PR)-positive cases, progestin has been used as a treatment with recurrent or disseminated disease with such characteristics. Most studies have employed oral progestogens, including medroxyprogesterone acetate (MPA), which have response rates in the range of 11% to 56% (2).

Unlike invasive endometrial cancer, the prognosis of well-differentiated endometrial cancer without myometrial invasion is excellent, with a 5-year survival rate of more than 90% (3). Therefore, younger patients with these noninvasive diseases can opt for progestin therapy instead of surgery if they wish to preserve their potential for fertility. Superior response rates ranging from 70% to 90% have been reported for progestin therapy in patients with such early stages of endometrial cancer or preinvasive hyperplasia (4, 5).

Despite the therapeutic utility of progestin to invasive and preinvasive endometrial neoplasia, the molecular mechanisms of progestin's inhibitor effects on endometrial glands are largely unknown. Initial studies have demonstrated that

Authors' Affiliations: [1]Department of Obstetrics and Gynecology, Kanazawa University Graduate School of Medical Science, Kanazawa, Ishikawa, Japan; [2]Virology Division, National Cancer Center Research Institute, Chuohku, Tokyo, Japan; [3]Pharmaceutical Research Center, Mochida Pharmaceutical Co., Ltd., Gotemba, Shizuoka, Japan; and [4]Department of Gynecology, Kyoundo Hospital, Sasaki Institute, Tokyo, Japan

Corresponding Author: Satoru Kyo, 13–1, Takaramachi, Kanazawa, Ishikawa 920–8641, Japan. Phone: 81-76-265-2425; Fax: 81-76-234-4266; E-mail: satoruky@med.kanazawa-u.ac.jp

American Association for Cancer Research

Translational Relevance

Endometrial cancer patients with recurrence at distant sites after initial surgery have few options for systemic therapy. Progestin [medroxyprogesterone acetate (MPA)] has been frequently used for such patients. Furthermore, younger patients with early stage endometrial cancer or endometrial hyperplasia can opt for progestin therapy instead of surgery if they wish to preserve their potential for fertility. However, efficacy of MPA varied among patients and no predictive parameter has been known, mainly due to lack of knowledge on the molecular mechanisms of progestin action to inhibit endometrial cell growth.

Our *in vitro* and *in vivo* treatment model has revealed that progestin directly induces FOXO via transcriptional activation to inhibit the growth of cancer and precancerous endometrial epithelial cells, indicating that FOXO is a novel target of MPA therapy, and Akt signaling, an upstream inhibitor of FOXO, is a potential predictor of MPA efficacy. This information will help define patient selection for progestin therapy.

progestin activates p21/WAF-1 expression, triggering cell cycle inhibition; therefore, p21/WAF-1 is a key effector of progestin action (6, 7). However, most studies have used breast cancer cell lines, whose response to progestin must be different from that of endometrial cells; for example, unlike endometrial cells, progestin occasionally has growth stimulatory effect on breast cancer cells *in vitro* and *in vivo*. Furthermore, either overexpression of ckd4 and/or cyclin D or dysfunction has been reported to frequently occur in a significant proportion of hormone-sensitive endometrial cancer, opposing p21/WAF-1 function (8–10), indicating that the p21/WAF-1 pathway is disrupted in endometrial carcinogenesis, and factors other than p21 may play crucial roles in exerting progestin action.

We have aimed to establish an *in vitro* and *in vivo* treatment model of progestin using immortalized and transformed endometrial epithelial cells expressing PR, and investigated the molecular mechanisms of progestin to inhibit the growth of endometrial glands. The microarray analyses identified the genes upregulated by progestin treatment, among which we noticed that the forkhead box O1 (*FOXO1*) gene plays a pivotal role in the progestin-mediated growth inhibition of the endometrial gland.

Experimental Procedures

Endometrial epithelial cell lineage and cell culture

EM-E6/E7/TERT cells are immortalized endometrial epithelial cells established by retroviral transduction of human papilomavirus (HPV) *E6/E7* genes together with human telomerase reverse transcriptase *(hTERT)* cDNA into primary endometrial epithelial cells purified from surgical specimens (11). EM-E6/E7/TERT/RAS cells are transformed cells with tumorigenicity in mice established

by the additional introduction of oncogenic mutant *K-ras* alleles into EM-E6/E7/TERT cells (12). Although parental EM-E6/E7/TERT cells constitutively express weak levels of PR, EM-E6/E7/TERT or EM-E6/E7/TERT/RAS cells were further transfected with retroviral progesterone receptor B (PRB) expression vector (MSCVbsd-PRB) so that these transfectants, named EM-E6/E7/TERT/PR or EM-E6/E7/TERT/RAS/PR cells, strongly and stably expressed PRB (Fig. 1A). Akt signaling is one of the major inhibitory pathways for FOXO1 activity. To clarify the role of FOXO1 as a target of progestins, we introduced dominant negative alleles of Akt (*DN-Akt*) by retroviral transfer (12) into EM-E6/E7/TERT/PR cells to establish EM-E6/E7/TERT/PR/DN-AKT cells. These endometrial epithelial cell lines were basically maintained in Dulbecco's modied Eagle's medium (DMEM) supplemented with 10% fetal bovine serum (FBS) in an atmosphere of 5% CO_2 at 37°C. Tumorigenic endometrial epithelial cells were maintained in DMEM with 10% FBS. MCF-7 (Michigan Cancer Foundation-7) cells were purchased from the American Type Culture Collection and used as a positive control for progesterone receptor A (PRA) and PRB expressions. Ishikawa cells were kindly provided by Dr. Masato Nishida (National Kasumi-gaura Hospital, Tsuchiura, Japan).

RT-PCR assay

The expression of p21/WAF-1, PRB, and FOXO1 mRNAs was analyzed by reverse transcriptase-PCR (RT-PCR) amplification. The primer pairs used were: 5'-CCTCTTCGG-CCCAGTGGAC-3' (forward),
5'–CCGTTTTCGACCCTGAGAG-3' (reverse) for *p21/WAF-1*,
5' – ACAGAATTCATGACTGAGCTGAAGGCAAAGGGT - 3' (forward),
5' – ACAAGATCTCAAACAGGCACCAAGAGCTGCTGA - 3' (reverse) for *PRB* (744–1173, 429 bp) (13),
5'–TGGACATGCTCAGCAGACATC-3' (forward),
5'-TTGGGTCAGGCGGTTCA-3' (reverse) for *FOXO1*.

For the detection of FOXO1 mRNA, EM-E6/E7/TERT or EM-E6/E7/TERT/PR cells were cultured in growth medium for 24 h and then incubated with or without MPA (10 nM) for different time periods. To examine whether FOXO1 mRNA expression depended on *de novo* protein synthesis, cycloheximide was simultaneously added with MPA at a final concentration of 10 µg/mL. Total RNA was then isolated from the cells using Isogen (Nippon Gene) according to the manufacturer's protocol, and cDNA was synthesized from 1 µg of RNA using the RNA PCR kit version 2 (TaKaRa) with random primers. Typically, 2 µL aliquots of the reverse-transcribed cDNA were amplified by 28 cycles of PCR in 50 µL of 1× buffer [10 mM Tris-HCl (pH 8.3), 2.5 mM $MgCl_2$, and 50 mM KCl] containing 1 mM each of dATP, dCTP, dGTP, and dTTP, 2.5 units of Gene Taq (Nippon Gene), and 0.2 µM primers. Each cycle consisted of denaturation at 94°C for 30 s, annealing at 52°C for 30 s, and extension at 72°C for 45 s for p21/WAF-1 or FOXO1, or at 94°C for 1 min, annealing at 56°C for 1 min, and extension at 72°C for 1 min for PRB or PRAB. The PCR products were resolved by electrophoresis
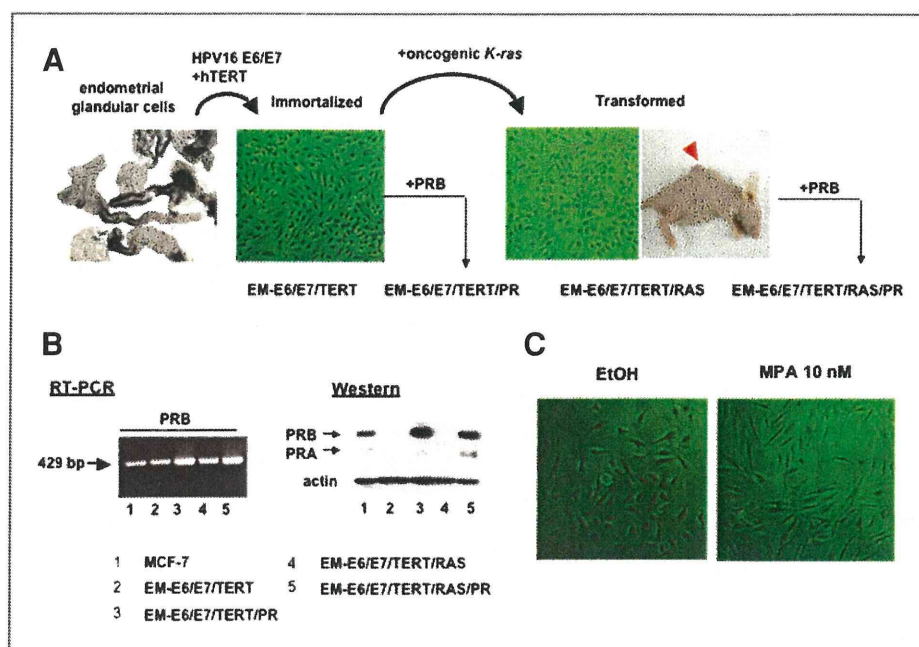
Figure 1. Endometrial epithelial cell lines used in the study. A, EM-E6/E7/TERT cells were immortalized cells generated from primary endometrial epithelial cells by the introduction of *HPV16 E6/E7* and *hTERT* genes (11). EM-E6/E7/TERT/RAS cells were generated from EM-E6/E7/TERT cells by the retroviral introduction of oncogenic mutant *K-ras* alleles, which produced transformed phenotypes, including anchorage-independent growth and tumorigenicity on nude mice (12). EM-E6/E7/TERT or EM-E6/E7/TERT/RAS cells were retrovirally transfected with *PRB* expression vector to achieve higher levels of PR expression. B, RT-PCR and western blot analyses were performed to confirm the expression of PR subtypes. PRA is an isoform of PR, lacking the N-terminal 164 amino acids of the larger isoform, PRB. The RT-PCR primers were designed to generate PRB products (429 bp) (15). The antibody against PR used in the western blot analysis recognized both PRA (81 kDa) and PRB (116 kDa), distinguishing each isoform by band size. MCF-7 cells were used as a positive control for PRA and PRB. C, change in cell shape of EM-E6/E7/TERT/PR cells following treatment with MPA for 72 h. Cells treated with MPA exhibited thinner and longer morphology.

on 7% polyacrylamide gels and stained with SYBR green I (FMC BioProducts). The efficiency of cDNA synthesis from each sample was estimated by PCR using glyceraldehyde 3 phosphate dehydrogenase (GAPDH)-specific primers as described previously (14).

Cell growth assay

Cells precultured in growth media for 24 h were incubated in 6-well plates in growth media or in serum-depleted media with phenol red-free DMEM in the absence or presence of MPA (MPA; 10 nM) or progesterone (10 nM), and cell growth was evaluated by counting the number of cells or measuring the incorporation of 5-Bromo-2′-deoxyuridine (BrdU) on the indicated days. The BrdU incorporation was detected using the DELFIA cell proliferation kit (PerkinElmer) according to the manufacturer's protocol as previously reported (15). EtOH was added so that its concentration was normalized to 0.1% in control and MPA- or progesterone-treated samples.

Cell cycle analysis

EM-E6/E7/TERT/PR cells were cultured in growth media in 6-well plates to 70%–80% confluence; then the media were replaced with serum-depleted phenol red-free DMEM and incubated for 24 h in the absence or presence of MPA

at 10 nM. The cells were harvested and fixed overnight with 3 mL of ice-cold 80% ethanol. The fixed cells were then centrifuged, suspended in lysis buffer (100 mmol/L sodium citrate and 0.1% Triton X-100), and incubated for 15 min at room temperature before incubating with RNase A (10 mg/mL; Sigma Chemical) for 10 min at room temperature. DNA was stained with propidium iodide (50 μg/mL) for at least 1 h at 4°C. The DNA content was determined by flow cytometry (Beckman Coulter) and EXPO 32 software.

Western blot analysis

For examining PRA and PRB expressions, nuclear extracts were prepared from EM-E6/E7/TERT, EM-E6/E7/TERT/PR, EM-E6/E7/TERT/RAS, or EM-E6/E7/TERT/RAS/PR cells as previously described (16). For examining p21/WAF-1, PTEN, p-AKT, or FOXO1 expression, EM-E6/E7/TERT or EM-E6/E7/TERT/PR cells preincubated in growth media for 24 h were incubated in serum-depleted phenol red-free DMEM in the absence or presence of MPA or progesterone (10 or 100 nM) for various time periods; whole-cell extracts or nuclear or cytoplasmic extracts were prepared as previously described (16). Fifteen micrograms of the nuclear extracts or 50–100 μg of whole-cell or cytoplasmic extracts were electrophoresed on a SDS-polyacrylamide gel and transferred to polyvinylidine difluoride membranes.

Membranes were blocked by immersion in TBST [150 mM NaCl, 20 mM Tris-Cl (pH 7.5), 0.1% Tween] containing 5% non-fat dried milk. They were then incubated with a specific antibody against PR [Progesterone Receptor Ab-8 (clone hPRa2+hPRa3); Lab Vision], p21/WAF (SC-469; Santa Cruz Biotechnology), PTEN [ABM-2052 (clone 6H2.1); Cascade BioScience], p-AKT (#4058; Cell Signaling Technology), or FOXO1 (#2880, Cell Signaling Technology). Next, the membranes were reacted with horseradish-peroxidase–conjugated anti-rabbit immunoglobulin (Jackson Immunoresearch Laboratories). The membranes were also probed with anti-actin antibody (Sigma) to normalize the differences among the samples. The LAS3000 CCD-Imaging System (Fujifilm Co. Ltd.) was used for detection and quantification of proteins visualized by Lumi-Light^{Plus} Western Blotting Substrate (Roche).

Nude mice xenograft experiments

EM-E6/E7/TERT/RAS or EM-E6/E7/TERT/RAS/PR cells were resuspended in a Hanks' balanced salt solution (Sigma) and subcutaneously injected (5×10^5 cells/mouse) at the base of the left flank of female 7- to 9-week-old ovariectomized BALB/c nu/nu mice (SLC). When tumors were seen after 3 weeks, hormone pellets consisting of placebo or progesterone (200 mg/pellet, 60-day release) (Innovative Research of America) were placed subcutaneously into the backs of the mice. Blood samples were collected from the tail vein, 10–14 days after pellet implantation, for measuring serum concentration of progesterone by ELISA (SRL, Inc.). Tumors were then monitored weekly for growth and were collected 4 weeks after pellet implantation. Half of the collected samples were stored for histological analysis after formalin fixation, while the other half were stored at −70°C until protein extraction.

Immunocytochemistry and immunohistochemistry

EM-E6/E7/TERT/PR cells were cultured on LAB TEK chamber slides (Nalge Nunc International) for 24 h and treated with or without MPA (10 nM) for 24 h. Then, the cells were fixed with 10% formaldehyde neutral buffer solution (37152-51; Nacalai Tesque, Inc.), immersed in methanol for 10 min at −20°C, blocked with PBS containing 10% goat serum and 0.3% Triton X-100 (166-11805; Wako Pure Chemical Industries, Ltd.) for 1 h at room temperature, and stained with monoclonal antibody to FOXO1 (#9462; Cell Signaling Technology) at 1:100 dilution for 12 h at 4°C. Next, they were incubated with fluorescent anti-rabbit IgG conjugates [Alexa Fluor 568 goat anti-rabbit IgG (H+L) highly cross-adsorbed, A11036; Invitrogen] for 1 h at room temperature in the dark. Cells were stained with 4′,6-diamidino-2-phenylindole (DAPI) (D1306; Invitrogen) for 3 min. Representative images were captured with a fluorescent microscope (Olympus BX-50; Olympus).

Immunohistochemical analysis was performed using formalin-fixed, paraffin-embedded specimens from mouse tumors formed with EM-E6/E7/TERT/RAS/PR cells. Sections were stained with a monoclonal antibody to FOXO1 (#9462; Cell Signaling Technology) at a 1:100 dilution for 12 h at 4°C. After the specimens were deparaffinized in xylene and graded alcohols, epitope retrieval was performed, in which the sections were heated in a microwave oven at 700 W for 10 min in 1× Antigen Retrieval Solution (Biogenex). Then, endogenous peroxidase was blocked by immersing the sections in 0.3% H_2O_2 methanol for 30 min. The reaction was visualized with the EnVision Detection Kit (DAKO Cytomedion) using diaminobenzidine tetrahydrochloride as the enzyme substrate. All sections were counterstained with GM hematoxylin stain solution (Muto Pure Chemicals Co., Ltd.). For negative controls, the non-reactive rabbit immunoglobulin fractions (X0903; Daco) or mouse IgG2a (X0943; Daco) was used, instead of the primary FOXO1 or cytokeratin antibodies, respectively.

DNA microarray analysis

For MPA-responsive gene expression profiling, EM-E6/E7/TERT/PR cells were cultured in growth medium for 24 h and then incubated with or without 10 nM MPA for 24 h.

The Agilent Whole Human Genome Oligo Microarrays (G4112A) containing 44,000 60-mer oligonucleotide probes representing 41,000 unique genes and transcripts were used for the experiments. Two types of total RNA samples were prepared: total RNA samples extracted from cells after 24 h with or without MPA treatment. Sample labeling and microarray processing was performed as detailed in the "One-Color Microarray-Based Gene Expression Analysis" (version 1.0, part number G4410-90040) protocol. Briefly, the Agilent One-Color Spike-Mix (part number 5188-5282) was diluted to 5,000-fold and 5 L of the diluted spike-in mix was added to 500 ng of each of the total RNA samples prior to labeling reactions. The spike-in mix consists of a mixture of 10 in vitro synthesized, poly-adenylated transcripts derived from the adenovirus E1A gene. The labeling reactions were performed using the Agilent Low RNA Input Linear Amplification Kit (part number 5183-3523) in the presence of cyanine 3-CTP (Perkin Elmer part number NEL 580). For microarray hybridization, 500 ng of cyanine-3-labeled cRNA was fragmented and hybridized on the Agilent Whole Human Genome microarrays at 65°C for 17 h using the Agilent Gene Expression Hybridization Kit (part number 5188-5242). The hybridized microarrays were dissembled at room temperature in Gene Expression Wash Buffer 1 (part number 5188-5325), and then washed in the same buffer at room temperature for 1 min. This was followed by a 1-min wash in Gene Expression Wash Buffer 2 (part number 5188-5326) at an elevated temperature. The processed microarrays were scanned with the Agilent DNA microarray scanner (part number G2565BA) and extracted with Agilent Feature Extraction software (version 8.5, part number 2567AA). The resulting text files were loaded into the Agilent GeneSpring GX software (version 7.3) for further analysis.

The microarray data set was normalized in GeneSpring GX using the following scheme: First, data transformation:

Intensity measurements less than 0.01 were set to 0.01. Second, per-chip normalization: Normalize to 70 percentile. Each intensity measurement on a microarray was divided by the 70-percentile intensity of all measurements on that microarray. Per-chip normalization removes any systemic error in signal intensities between chips. Third, per-gene normalization: Normalize to specific samples. For each gene, intensity values in all samples were normalized to the intensity value for that gene in the control samples. Per-gene normalization was carried out to investigate the relative gene expression of each sample after MPA treatment compared with specific control samples. We compared microarray data between samples with and without MPA treatment. Microarray data are supplied on our Supplemental Materials site.

Luciferase reporter assay

The 2.0 kb 5′-upstream region of the *FOXO1* gene (-1993 to -18: numbering based on the first ATG of *FOXO1* gene) was PCR-amplified from genomic DNA using primer set, 5′-CTAATTTTTCCTTTTTTCCCCTC-3′ (forward) and 5′-AGGGGCGGGGGTCACC-3′ (reverse), and inserted into the luciferase reporter plasmid pGL3-basic (Promega), named p-FOXO1-pro. EM-E6/E7/TERT/PR cells preincubated in growth media in 24-well dishes for 24 h were incubated in serum-depleted phenol red-free DMEM and transfected with 0.4 μg of reporter plasmid using Lipofectamin PLUS (Invitrogen Corp.) according to the manufacturer's protocol. Cells were simultaneously treated with 10 nM MPA for 48 h before being harvested and cell extracts prepared. Luciferase assays were performed using the Dual-Luciferase Reporter Assay System (Promega), in which Renilla luciferase plasmids were cotransfected as controls to standardize transcription efficiency. All experiments were performed at least three times for each plasmid, and the relative luciferase activity reported here is the mean of the three results.

siRNA inhibition assay

EM-E6/E7/TERT/PR cells were seeded overnight in the growth media in 6-well plates and transfected the next day with 25 nmol/L of non-specific scramble siRNA$_{control}$ (Ambion) or FOXO1A-specific siRNA (Ambion) using Lipofectamine 2000 reagent (Invitrogen) according to the manufacturer's recommendations. Forty-eight hours after transfection, cells were incubated in serum-depleted phenol red-free DMEM in the absence or presence of 10 nM MPA for 72 h before the cell number was counted in each sample to evaluate the effects of MPA on cell growth.

Statistical analysis

The data were basically presented as the mean ± SD of triplicated assays. Differences between groups were evaluated using Student's *t*-test. A *P* value of less than 0.05 was considered to indicate statistical significance.

Results

Progestin inhibits the growth of endometrial epithelial cell lines without p21/WAF-1 induction

We have previously established immortalized endometrial epithelial cells (EM-E6/E7/TERT cells) (Fig. 1A) (11) that sustain the functional characteristics of primary cells, including steroid responsiveness; estrogen treatment promoted cell growth *in vitro* whereas progestin treatment inhibited it, although these responsiveness weakened with increased population doublings. Tumorigenic endometrial epithelial cells (EM-E6/E7/TERT/RAS) were established by the additive introduction of oncogenic *mutant K-RAS* alleles into EM-E6/E7/TERT cells, which have the potential to form colonies on soft agar and tumors on nude mice (12). Basically, these immortal and transformed cells express weak levels of estrogen receptor α (ERα) as well as PR. To enhance the effect of progestin, stable cell lines expressing higher levels of PR were established by the additive introduction of *PRB* cDNA into immortal and transformed cells, named EM-E6/E7/TERT/PR and EM-E6/E7/TERT/RAS/PR cells, respectively. The expression of PR was then confirmed in these cells. RT-PCR assays confirmed that all these immortal cells expressed PRB. Western blot analysis revealed that EM-E6/E7/TERT/PR or EM-E6/E7/TERT/RAS/PR cells exhibited high levels of PRB expression with weak or faint levels of PRA expression (Fig. 1B), as shown in our recent study (15).

We first examined the effect of progestin on these cells *in vitro*. EM-E6/E7/TERT/PR or EM-E6/E7/TERT/RAS/PR cells were cultured in growth media and treated with 10 nM MPA for different time periods and the cell growth was monitored. The cells exhibited a longer and thinner morphology by the treatment with MPA (Fig. 1C). Significant growth retardation was observed after 4–5 days of treatment (Fig. 2A and B). In contrast, cells without PR overexpression (EM-E6/E7/TERT/vec or EM-E6/E7/TERT/RAS/vec) lacked the inhibitory effect of MPA (Fig. 2C and D), indicating that the growth inhibition was PR-dependent. We also confirmed MPA responsiveness in serum-depleted conditions as well (Supplementary Fig. 1). Significant growth inhibition was similarly observed in cells with PR overexpression but not those without it, although the extent of inhibition was lesser than cells incubated in growth media, probably because decreased proliferative activity by serum depletion masked the inhibitory effect of MPA. Furthermore, we tested the effect of another progestin, progesterone, on these cells. Progesterone inhibited the growth of EM-E6/E7/TERT/PR or EM-E6/E7/TERT/RAS/PR cells in a similar fashion (Fig. 2E and F) but not EM-E6/E7/TERT/vec or EM-E6/E7/TERT/RAS/vec cells (data not shown). Flow cytometric analysis revealed that MPA increased G0/G1 fractions by 5% to 6% and sub-G0/G1 fractions by 1% to 2% (Supplementary Fig. 2). To examine whether or not p21/WAF-1 was involved in MPA-induced growth retardation, we measured the change in p21/WAF-1 expression on treatment with MPA. RT-PCR assays or western blot analysis revealed that there was no

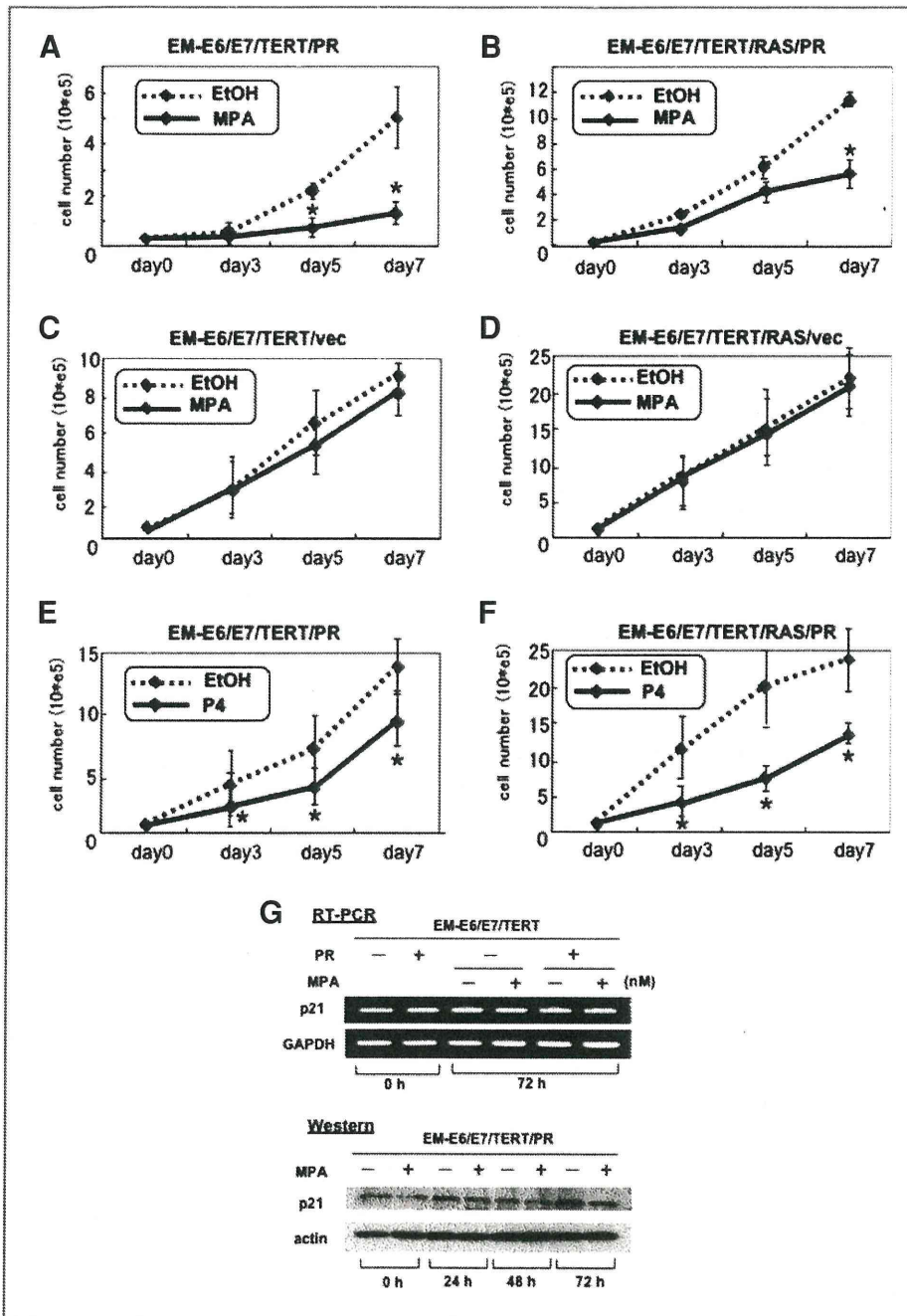Figure 2. *In vitro* effect of progestin on the growth of endometrial epithelial cell lines. *In vitro* growth assay of endometrial epithelial cell lines treated with MPA or progesterone (P4). Cells were grown in growth media with or without 10 nM MPA (A–D) or progesterone (E and F) for different time periods; cell growth was determined by counting the cell number for each period. Note that MPA as well as progesterone significantly inhibited the growth of cells with PRB overexpression (A, B, E, and F) but not those without it (C and D). Each point represents the means ± SD of triplicate determinations in three independent experiments. *$P <$ 0.05. G, analyses of the p21 expression upon MPA stimulation. EM-E6/E7/TERT or EM-E6/E7/TERT/PR cells were treated with or without MPA at 10 nM at different time periods, and RT-PCR and western blot analyses were performed.

significant induction of p21/WAF-1 mRNA or protein expression (Fig. 2G). Thus, p21/WAF-1 does not appear to play critical role in MPA-induced growth retardation.

We then examined the *in vivo* effects of progestin on the growth of tumorigenic endometrial cells. EM-E6/E7/TERT/RAS/PR cells were implanted to the flank of nude mice, and then progesterone pellets were inoculated after 3 weeks. Progesterone rather than MPA was selected because it is easy to measure its serum concentration using our available kit. As expected, progesterone concentration was significantly higher in treated groups than untreated groups [39.5 (15.1–73.2) vs. 7.5 (2.8–9.2) ng/mL, respectively]. As shown in Figure 3, tumors significantly decreased in size in treated groups. Taken together, these findings clearly show that progestin exerted an inhibitory effect on the cell growth of endometrial epithelial cell lineages both *in vitro* and *in vivo* in a p21/WAF-1–independent manner.

Figure 3. *In vivo* effect of MPA on the growth of endometrial epithelial cell lines. EM-E6/E7/TERT/RAS/PR cells were inoculated on the flank of mice. After tumor growth was confirmed, control placebo pellets or progesterone pellets were administrated subcutaneously, and then tumor growth was monitored. Mean serum concentration of progesterone was shown for each group. Data are presented as mean ± SD; *$P <$ 0.05.
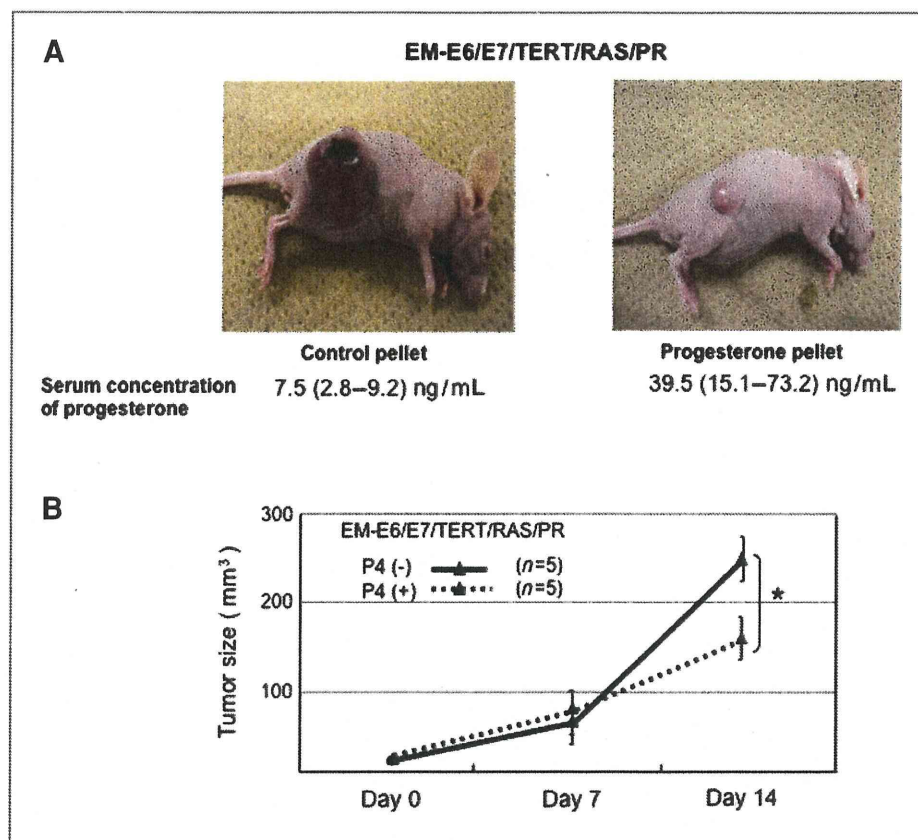
Progestin induces FOXO1 expression via transcriptional activation in endometrial epithelial cell lines

To identify the molecular mechanisms of progestin's growth inhibitory effect on endometrial epithelial cell lines, we compared gene expression profiles of EM-E6/E7/TERT/PR cells treated and untreated with MPA. Of 44,000 transcripts included in the DNA microarray, we first defined the genes induced more than 10-fold by MPA stimulation and identified 24 of them (Supplementary Table 1). Of these genes, we noticed the *FOXO1* gene, because previous studies have found that progestin regulates the expression of *FOXO1* in endometrial stromal cells through subcellular translocation linked to its phosphorylation status, triggering endometrial decidualization and menstruation (17).

We therefore examined the change in expression and subcellular localization of FOXO1 in endometrial epithelial cell lines following treatment with progestin. EM-E6/E7/TERT or EM-E6/E7/TERT/PR cells were treated with MPA and western blot analyses performed using FOXO1-specific antibody. FOXO1 expression was significantly induced by treatment with MPA as well as progesterone at 10 or 100 nM in EM-E6/E7/TERT/PR cells (Fig. 4A) but not EM-E6/E7/TERT cells (data not shown). Induction was mainly observed in the nuclei, with only

weak or faint levels of FOXO1 expression in the cytoplasm. Immunocytochemical analysis using EM-E6/E7/TERT/PR cells clearly showed that FOXO1 was mainly induced in the nuclei by MPA (Fig. 4B). Thus, progestin facilitates FOXO1 expression in a PR-dependent manner *in vitro*. This was not due to a change in the subcellular localization of FOXO1 (from cytoplasm to nucleus) because no significant FOXO1 expression was observed in the cytoplasm of untreated cells (Fig. 4A).

We then confirmed the induction of FOXO1 expression *in vivo* by the treatment with progesterone. Mouse tumors of EM-E6/E7/TERT/RAS/PR cells treated or untreated with progesterone pellets were collected and subjected to western blot analysis. As shown in Figure 4C, FOXO1 protein expression was upregulated by progesterone treatment in tumor tissues. Immunohistochemistry also showed that tumors exhibited marked induction of FOXO1 mainly in the nuclei when treated with progesterone (Fig. 4C).

We investigated the molecular mechanisms of FOXO1 induction upon MPA treatment. RT-PCR analysis was performed for FOXO1 mRNA expression using EM-E6/E7/TERT/PR cells treated or untreated with MPA. FOXO1 mRNA was significantly upregulated 8–72 h after the treatment (Fig. 5A). This activation was not blocked by treatment with cycloheximide, indicating that MPA directly activates FOXO1 mRNA expression without *de novo* protein
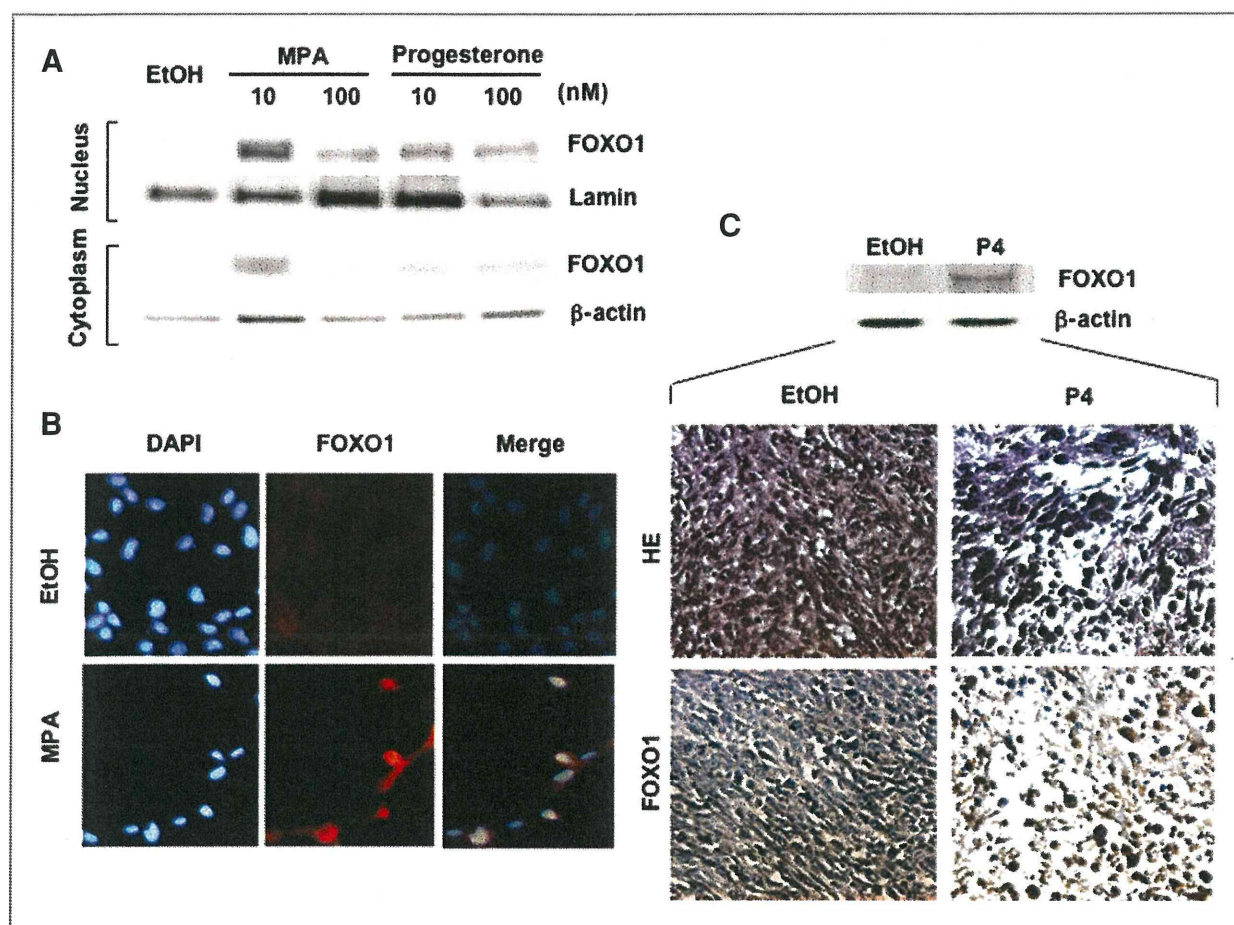
Figure 4. Induction of FOXO1 by progestin. A, EM-E6/E7/TERT/PR cells preincubated in growth media for 24 h were incubated in the serum-depleted phenol red–free DMEM in the absence or presence of MPA or progesterone for 48 h at the indicated concentrations. Nuclear or cytoplasmic extracts were collected from cells and the western blot analysis was performed using FOXO1 antibody. Lamin and β–actin were used as controls for nuclear or cytoplasmic protein loading, respectively. B, immunocytochemistry of FOXO1. EM-E6/E7/TERT/PR cells preincubated in growth media for 24 h were incubated on LAB TEK chamber slides for 24 h in the absence or presence of MPA for 24 h. After fixation, the cells were incubated with primary antibody to FOXO1, followed by fluorescent anti-IgG secondary antibody. The cells were also incubated with DAPI for nuclear staining and observed under a fluorescence microscope. Note that FOXO1 expression is induced preferentially in the nuclei (consistent with DAP staining) by MPA treatment. D, mouse tumors formed with EM-E6/E7/TERT/RAS/PR cells were treated with or without progesterone (P4) via subcutaneous injection of hormone pellets and were collected 4 weeks after the treatment. Then, whole-cell extracts were prepared, followed by western blot analysis for FOXO1. Immunohistochemistry of FOXO1 was also performed with matched samples of the EM-E6/E7/TERT/RAS/PR tumors treated with or without P4. HE staining of the tumor samples and induced FOXO1 expression mainly in the nuclei of the tumor cells are shown.

synthesis. We confirmed that this activation was not obvious in cells lacking PR-overexpression (EM-E6/E7/TERT cells) (Fig. 5A), suggesting that FOXO1 activation by MPA is PR-dependent. We further performed the luciferase reporter assays using FOXO1 gene promoter spanning 2.0 kb sequences upstream of the first ATG. As shown in Figure 5B, MPA treatment of EM-E6/E7/TERT/PR cells activated the FOXO1 promoter approximately by 3-fold, while no activation was observed in EM-E6/E7/TERT cells. These findings indicate that MPA directly induces FOXO1 expression via the transcriptional activation of FOXO1. To analyze the status of signaling pathway, which regulates subcellular localization of FOXO1, we examined the

expression of PTEN and p-AKT as critical components of phosphatidylinositol 3-kinase (PI3K)/AKT pathway. As shown in Figure 5C, activation of PTEN expression or reduction of p-AKT expression, both of which facilitate nuclear retention of FOXO1, was not observed by the treatment with MPA.

FOXO1 mediates progestin to inhibit epithelial cell growth

To investigate the role of FOXO1 in the effect of progestin, a knockdown experiment for FOXO1 was performed via siRNA inhibition. EM-E6/E7/TERT/PR cells were transfected with siRNA against FOXO1 and treated
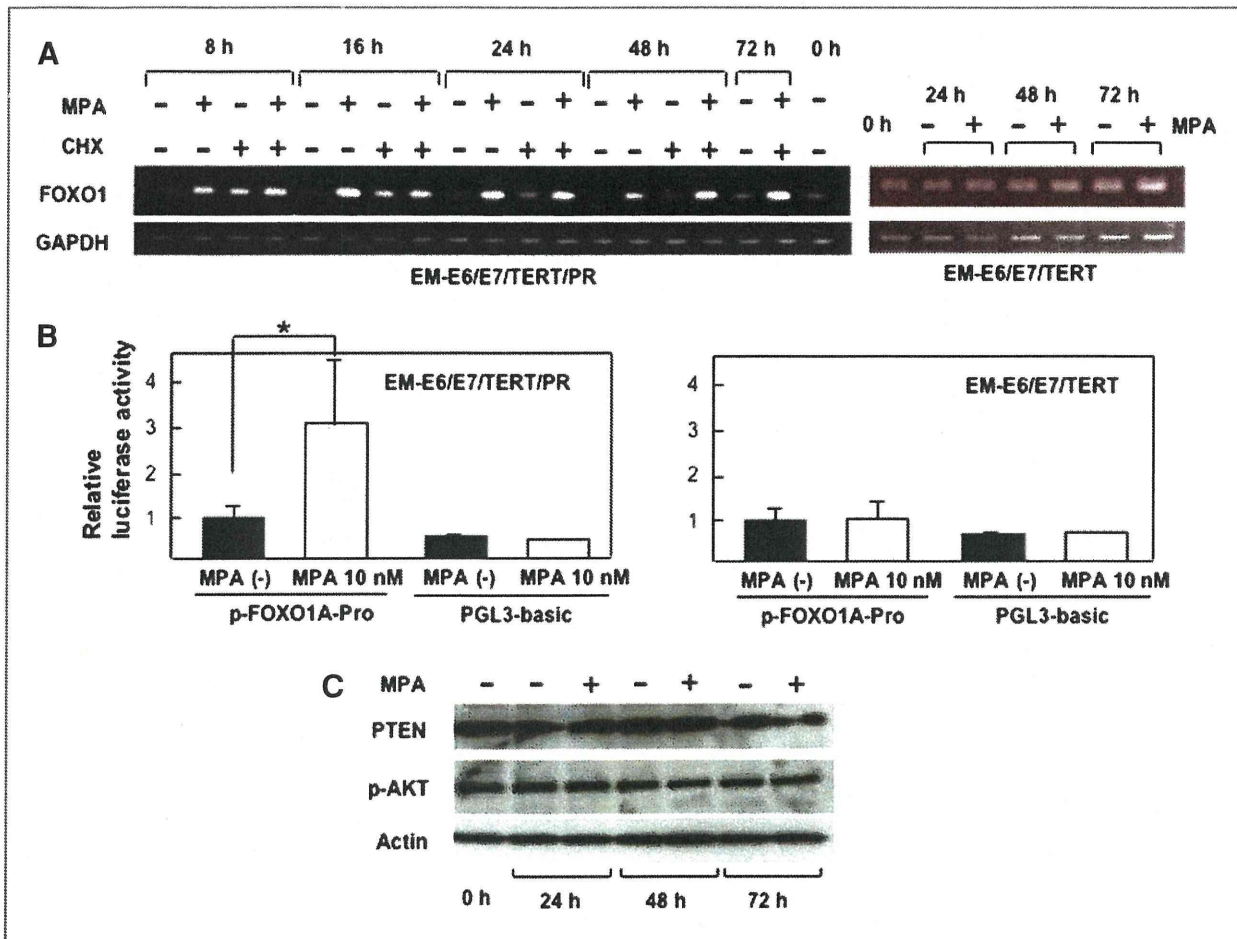
Figure 5. Mechanisms of FOXO induction by progestin. A, RT-PCR analysis of FOXO1 in EM-E6/E7/TERT/PR or EM-E6/E7/TERT cells. The cells were cultured with or without MPA in the presence or absence of cycloheximide (CHX) for different time periods and RNAs were collected and subjected to the RT-PCR for FOXO1. B, luciferase reporter assay using FOXO promoter. EM-E6/E7/TERT or EM-E6/E7/TERT/PR cells were transfected with luciferase reporter plasmid containing 2.0 kb of FOXO promoter or with blank reporter plasmid (pGL3-basic), followed by treatment with or without MPA. Seventy-two hours after treatment, cells were recovered and luciferase assays were performed. Relative luciferase activity is shown in each reporter plasmid. Data are presented as mean ± SD of the three independent experiments. *$P < 0.05$. C, EM-E6/E7/TERT/PR cells were treated with or without MPA at 10 nM and incubated at different time periods, followed by the western blot analysis for PTEN or p-AKT.

with or without MPA at 10 nM, followed by monitoring cell growth. Western blot analysis confirmed that knockdown was successful, exhibiting apparently decreased FOXO1 expression. These cells showed only minimally inducible FOXO1 expression on treatment with MPA (Fig. 6). In the absence of MPA, cells with knocked-down FOXO1 had increased growth rate compared with those with control siRNA, indicating that endogenous FOXO1 plays some role in cell proliferation. Treatment with MPA significantly inhibited the growth of cells transfected with control siRNA, while the inhibition was largely abrogated in those with knocked-down FOXO1. Thus, the effect of MPA was attenuated via knockdown of FOXO1, supporting the role of FOXO1 in progestin action. We sought to confirm whether similar effect was observed in other endometrial cancer cell lines as well. FOXO1 knockdown was performed in Ishikawa cells in the same way and MPA

effect was examined (Supplementary Fig. 3). Ishikawa cells exhibited growth inhibition as well as FOXO1 induction by the treatment with MPA, but with lesser extent, probably due to very low levels of PR expression. FOXO1 knockdown effectively cancelled growth inhibition by MPA.

Akt signaling limits progestin action on endometrial epithelial cell growth

FOXO family members are direct downstream targets of the PI3K/Akt signal transduction pathway. Activation of PI3K/Akt signals phosphorylates FOXO proteins, resulting in cytoplasmic retention and inhibiting their transcriptional activity. Therefore, we speculated that Akt signaling might affect the action of progestin. To investigate this possibility, a special cell line, named EM-E7/E7/TERT/PR/DN-AKT, was established with an introduced dominant
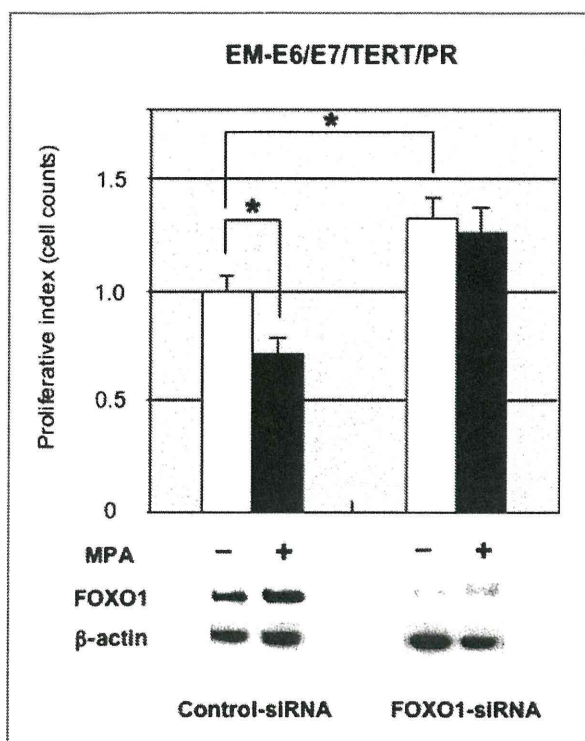
Figure 6. Role of FOXO1 in the action of progestin. EM-E6/E7/TERT/PR cells were transfected with non-specific scramble siRNA$_{control}$ or FOXO1-specific siRNA. Forty-eight hours after transfection, the cells were incubated with or without MPA at 10 nM for 72 h. Then, western blot analysis was performed to confirm the levels of FOXO1 expression. Simultaneously, cell number was counted in paired samples and shown as the relative value (proliferation index) in each sample to evaluate the effects of MPA. Data are presented as mean ± SD of the three independent experiments. *P < 0.05.

negative allele of *Akt* gene from EM-E7/E7/TERT/PR cells. Introduction of the dominant negative allele of *Akt* gene has been confirmed to inhibit Akt function in endometrial epithelial cell lines (12). Both cells exhibited similar growth rate in the absence of MPA (Fig. 7A). We then compared the effects of MPA on these cells. Treatment with MPA at 10 nM led to 35% growth inhibition of EM-E7/E7/TERT/PR/vector cells on day 3 and 46% on day 6 (Fig. 7A). The same treatment in EM-E7/E7/TERT/PR/DN-AKT cells resulted in 56% growth inhibition on day 3 and 66% on day 6. Thus, introducing DN-AKT caused enhanced growth inhibition by MPA.

We next examined the extent of FOXO1 induction by MPA in the nuclei of both cells (Fig. 7B). The western blot analysis revealed the enhanced FOXO1 induction in EM-E7/E7/TERT/PR/DN-AKT compared with EM-E7/E7/TERT/PR/vector cells on days 3 and 6. Especially, most prominent induction of FOXO1 was observed in EM-E7/E7/TERT/PR/DN-AKT on day 6, when the maximal growth inhibition was confirmed in Figure 7A. These findings proved that Akt signaling is a critical factor that limits the progestin action to endometrial epithelial cells.

Discussion

FOXO1 is a member of the FOXO subfamily of the Forkhead/winged helix family of transcription factors that is involved in cell cycle regulation and apoptosis (17): the subfamily contains the mammalian members FOXO1 (Fkhr), FOXO3a (Fkhr-l1), and FOXO4 (Afx) (18, 19). The role of FOXO1 in endometrial biology has been known in relation to the process of decidualization (17, 20, 21). FOXO1 induces the expression of decidualization-specific genes of endometrial stromal cells, such as insulin-like growth factor binding protein 1 (*IGFBP1*), decorin (*DCN*), and prolactin (*PRL*): this is enhanced by the action of cyclic AMP (camp). Here, we focused on the roles of FOXO1 in progestin action on endometrial epithelial cells and clearly showed it to be a novel target of progestin to inhibit the growth of both non-tumorigenic and tumorigenic endometrial epithelial cells.

The canonical pathway of FOXO1 regulation has been thought to be on the PI3K pathway. Growth-factor–dependent activation of the PI3K pathway blocks the function of all FOXO members by Akt-dependent phosphorylation of their three conserved residues, which leads to inhibition of DNA binding, nuclear exclusion, and subsequent sequestration in the cytoplasm (22–24). Recently, a unique role of progestin in the survival of endometrial stromal cells has been reported by Labied and colleagues (17). According to their results, progestin treatment of stromal cells enhanced the expression of phosphorylated FOXO1, which, because it is strictly localized to the cytoplasm, is considered to be an inactive form. Withdrawal of progestin induced rapid nuclear translocation of FOXO1, which activated expression of *BIM*, a known FOXO target gene encoding for a proapoptotic Bcl-2 homology 3 domain-only protein (25). This unique role of FOXO1 in response to progestin withdrawal was demonstrated in differentiating stromal cells of the endometrium. On the other side, we found that progestin induced FOXO1 expression mainly in the nuclei upon progestin stimulation in endometrial epithelial cells. RT-PCR assay clearly showed that FOXO1 mRNA is upregulated approximately 4–8 h after treatment with MPA, even in the presence of cycloheximide. Luciferase reporter assays demonstrated that MPA upregulated the transcriptional activity of *FOXO* promoter. Therefore, our results support the direct transcriptional activation of *FOXO1* gene by progestin. Computer-assisted homology search found potential PR-binding sites that have a homology with the glucocorticoid receptor-responsive element on the *FOXO1* promoter (data not shown). We are currently confirming the specific interaction of PR with such sites on the *FOXO* promoter. What is the molecular mechanism of the nuclear FOXO1 accumulation upon progestin stimulation? The most probable scenario might be that MPA inhibits PI3K/AKT signaling pathway, leading to the nuclear FOXO1 translocation. However, we confirmed that PI3K/AKT pathway was not inhibited by MPA in endometrial epithelial cells (Fig. 5D). Alternatively, it is known that FOXO1 binds to PR in the nuclei (26) and this physical

Figure 7. Akt activity limits the MPA effect. A, EM-E6/E7/TERT/PR/DN-AKT or EM-E6/E7/TERT/PR/vector cells were established from EM-E6/E7/TERT/PR cells by retroviral transfection of dominant negative *Akt* gene or blank vector, respectively. These cells were treated with or without MPA for different periods, and the cell number was counted to evaluate the proliferative activity. Data are presented as mean ± SD of the three independent experiments. B, western blot analysis was performed using nuclear extracts of EM-E6/E7/TERT/PR/DN-AKT or EM-E6/E7/TERT/PR/vector cells in the absence or presence of MPA on day 3 or day 6 to compare the levels of nuclear FOXO1 induction. Data are presented as mean ± SD of the three independent experiments.
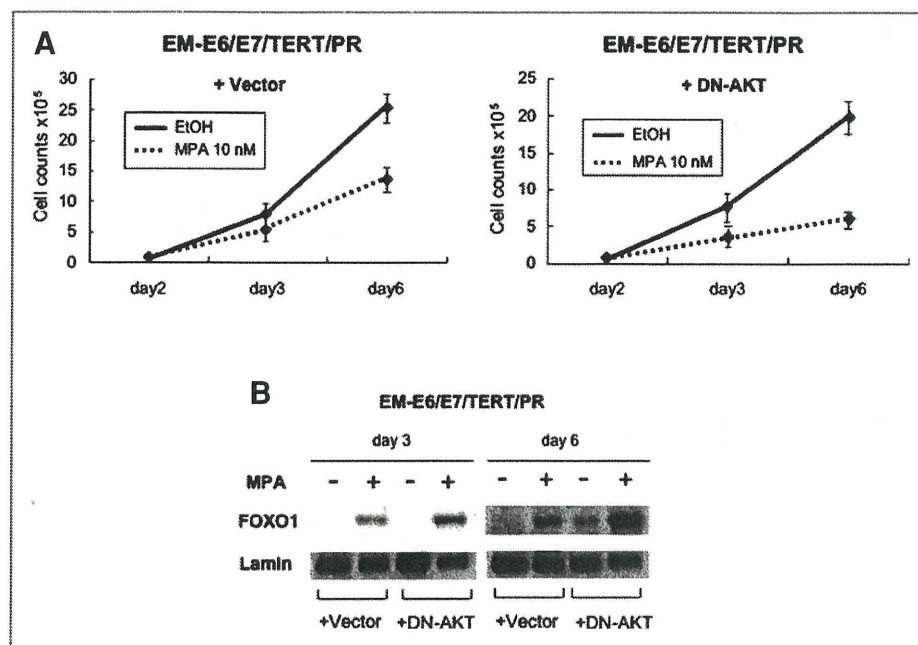
interaction may account for the nuclear accumulation. Further mechanistic study will be needed to clearly dissect molecular mechanisms of nuclear accumulation of FOXO1 by progestin in endometrial epithelial cells.

A role for FOXO1 in inhibiting cell growth has recently been reported using endometrial cancer cell lines *in vitro* (27). Overexpression of a gain-of-function mutant of the FOXO family inhibited the growth of Ishikawa cells that constitutively express low levels of FOXO1, while siRNA inhibition of the *FOXO* gene in HEC-1® cells that express high levels of FOXO1 enhanced their growth. Furthermore, Ward and colleagues also demonstrated that progestins increased FOXO1 protein levels in endometrial cancer cell lines, specifically through PRB (28), supporting our data. A growth inhibitory effect of FOXO family members has been proposed in other cell types, in particular, in vascular cells (29, 30). More recently, a role of the FOXO family as a tumor suppressor has been proposed (31). To circumvent embryonic lethality, Paik and colleagues used an inducible Cre-lox system to knock out the FOXO family: the widespread somatic deletion of these genes caused thymic lymphomas and hemangiomas, which were associated with increased cell proliferation and survival in these lineages (31). What are the downstream targets of FOXO for inhibiting cell growth? Recently, sprouty (Spry2), a negative regulator of receptor tyrosine kinases, was validated as a direct FOXO target to inhibit cell cycle progression and induce apoptosis (31). Several other forkhead-responsive genes have been reported, including Insulin-like growth factor-binding protein-1 (*IGBP-1*), glucose-6-phosphatase, FasL, Trail, and Bim (20, 25, 32–35). However, in DNA microarray and RT-PCR analyses, we failed to observe

upregulation of these candidate genes upon MPA stimulation (data not shown). Therefore, at present, it remains unclear how cell cycle arrest at G0/G1 is conferred by FOXO1 in endometrial epithelial cells.

In clinical practice of cancer treatment, we have no reliable parameter to predict the efficacy of MPA therapy. We found that the Akt signal, an upstream inhibitory factor of FOXO family, limits the effect of progestin. As we cannot predict the activation of FOXO by MPA before the treatment, the status of Akt activation could be an alternative predictor of MPA therapy. Our preliminary data show that patients responsive to MPA therapy have decreased p-AKT expression confirmed by immunohistochemistry in pretreated samples. It is well known that RAS signalings lead to AKT activation in various cancers via cross-talk signalings (36). It is therefore possible that activated RAS signalings (such as via *RAS* mutation) disturb MPA responsiveness and is an additional predictor of MPA therapy. In the present study, EM-E6/E7/TERT/RAS/PR cells with oncogenic *KRAS* mutation well responded to MPA (Figs. 2 and 3). These cells exhibit only weak levels of p-AKT expression, lacking AKT activation even with *KRAS* mutation (data not shown). Furthermore, in clinical samples, *KRAS* mutation is not always associated with AKT activation in endometrial cancer (37). Therefore, the status of *RAS* does not appear to be a strong predictor of MPA response, but this point requires further investigation.

In summary, our *in vitro* and *in vivo* treatment model has, for the first time, revealed that progestin targets FOXO via transcriptional activation to inhibit the growth of both non-transformed and transformed endometrial

epithelial cells without p21/WAF-1 induction. Further investigations of the FOXO1 target genes as well as of AKT signaling as a predictor of MPA efficacy are required to fully understand the molecular mechanisms of progestin effects and help define patient selection for progestin therapy.

Disclosure of Potential Conflicts of Interest

No potential conflicts of interest were disclosed.

References

1. Parkin DM, Bray F, Ferlay J, Pisani P. Global cancer statistics, 2002. CA Cancer J Clin 2005;55:74–108.
2. Moore TD, Phillips PH, Nerenstone SR, Cheson BD. Systemic treatment of advanced and recurrent endometrial carcinoma: current status and future directions. J Clin Oncol 1991;9:1071.
3. Creasman WT, Odicino F, Maisonneuve P, Beller U, Benedet JL, Heintz AP, et al. Carcinoma of the corpus uteri. J Epidemiol Biostat 2001;6:47–86.
4. Kaku T, Yoshikawa H, Tsuda H, Sakamoto A, Fukunaga M, Kuwabara Y, et al. Conservative therapy for adenocarcinoma and atypical endometrial hyperplasia of the endometrium in young women: central pathologic review and treatment outcome. Cancer Lett 2001; 167: 39–48.
5. Ushijima K, Yahata H, Yoshikawa H, Konishi I, Yasugi T, Saito T, et al. Multicenter phase II study of fertility-sparing treatment with medroxyprogesterone acetate for endometrial carcinoma and atypical hyperplasia in young women. J Clin Oncol 2007;25:2798–803.
6. Owen GI, Richer JK, Tung L, Takimoto G, Horwitz KB. Progesterone regulates transcription of the p21(WAF1) cyclin-dependent kinase inhibitor gene through Sp1 and CBP/p300. J Biol Chem 1998;273: 10696–701.
7. Migliaccio A, Piccolo D, Castoria G, Di Domenico M, Bilancio A, Lombardi M, et al. Activation of the Src/p21ras/Erk pathway by progesterone receptor via cross-talk with estrogen receptor. EMBO J 1998;17:2008–18.
8. Niemann TH, Yilmaz AG, McGaughy VR, Vaccarello L. Retinoblastoma protein expression in endometrial hyperplasia and carcinoma. Gynecol Oncol 1997;65:232–6.
9. Semczuk A, Miturski R, Skomra D, Jakowicki JA. Expression of the cell-cycle regulatory proteins (pRb, cyclin D1, p16INK4A and cdk4) in human endometrial cancer: correlation with clinicopathological features. Arch Gynecol Obstet 2004;269:104–10.
10. Enomoto T, Fujita M, Inoue M, Rice JM, Nakajima R, Tanizawa O, et al. Alterations of the p53 tumor suppressor gene and its association with activation of the c-K-ras-2 protooncogene in premalignant and malignant lesions of the human uterine endometrium. Cancer Res 1993; 53:1883–8.
11. Kyo S, Nakamura M, Kiyono T, Maida Y, Kanaya T, Tanaka M, et al. Successful immortalization of endometrial glandular cells with normal structural and functional characteristics. Am J Pathol 2003;163:2259–69.
12. Mizumoto Y, Kyo S, Ohno S, Hashimoto M, Nakamura M, Maida Y, et al. Creation of tumorigenic human endometrial epithelial cells with intact chromosomes by introducing defined genetic elements. Oncogene 2006;25:5673–82.
13. Akahira J, Inoue T, Suzuki T, Ito K, Konno R, Sato S, et al. Progesterone receptor isoforms A and B in human epithelial ovarian carcinoma: immunohistochemical and RT-PCR studies. Br J Cancer 2000;81: 1488–94.
14. Akahira J, Inoue T, Suzuki T, Ito K, Konno R, Sato S, et al. Telomerase activation by hTRT in human normal fibroblasts and hepatocellular carcinomas. Nat Genet 1998;18:65–8.
15. Shimizu Y, Takeuchi T, Mizuguchi K, Kiyono T, Inoue M and Kyo S. Dienogest, a synthetic progestin, inhibits the proliferation of immortalized human endometrial epithelial cells with suppression of cyclin D1 gene expression. Mol Hum Reprod 2009;15:693–701.
16. Schreiber E, Matthias P, Muller MM, Schaffner W. Rapid detection of octamer binding proteins with "mini-extracts," prepared from a small number of cells. Nucleic Acids Res 1989;17:6419.
17. Labied S, Kajihara T, Madureira PA, Fusi L, Jones MC, Higham JM, et al. Progestins regulate the expression and activity of the forkhead transcription factor FOXO1 in differentiating human endometrium. Mol Endocrinol 2006;20:35–44.
18. Accili D, Arden KC. FoxOs at the crossroads of cellular metabolism, differentiation, and transformation. Cell 2004;117:421–6.
19. Anderson MJ, Viars CS, Czekay S, Cavenee WK, Arden KC. Cloning and characterization of three human forkhead genes that comprise an FKHR-like gene subfamily. Genomics 1998;47:187–99.
20. Brunet A, Bonni A, Zigmond MJ, Lin MZ, Juo P, Hu LS, et al. Akt promotes cell survival by phosphorylating and inhibiting a forkhead transcription factor. Cell 1999;96:857–68.
21. Buzzio OL, Lu Z, Miller CD, Unterman TG, Kim JJ. FOXO1A differentially regulates genes of decidualization. Endocrinology 2006;147: 3870–6.
22. Grinius L, Kessler C, Schroeder J, Handwerger S. Forkhead transcription factor FOXO1A is critical for induction of human decidualization. J Endocrinol 2006;189:179–87.
23. Lin K, Dorman JB, Rodan A, Kenyon C. daf-16: an HNF-3/forkhead family member that can function to double the life-span of Caenorhabditis elegans. Science 1997;278:1319–22.
24. Kops GJ, de Ruiter ND, De Vries-Smits AM, Powell DR, Bos JL, Burgering BM. Direct control of the forkhead transcription factor AFX by protein kinase B. Nature 1999;398:630–34.
25. Dijkers PF, Medema RH, Lammers JW, Loenderman L, Coffer PJ. Expression of the pro-apoptotic Bcl-2 family member Bim is regulated by the forkhead transcription factor FKHR-L1. Curr Biol 2000;10: 1201–04.
26. Takano M, Lu Z, Goto T, Fusi L, Higham J, Francis J, et al. Transcriptional cross talk between the forkhead transcription factor forkhead box O1A and the progesterone receptor coordinates cell cycle regulation and differentiation in human endometrial stromal cells. Mol Endocrinol 2007;21:2334–49.
27. Goto T, Takano M, Albergaria A, Briese J, Pomeranz KM, Cloke B, et al. Mechanism and functional consequences of loss of FOXO1 expression in endometrioid endometrial cancer cells. Oncogene 2008;27:9–19.
28. Ward EC, Hoekstra AV, Blok LJ. The regulation and function of the forkhead transcription factor, forkhead box O1, is dependent on the progesterone receptor in endometrial carcinoma. Endocrinology 2008;149:1942–50.
29. Potente M, Urbich C, Sasaki K, Hofmann WK, Heeschen C, Aicher A, et al. Involvement of Foxo transcription factors in angiogenesis and postnatal neovascularization. J Clin Invest 2005;115:2382–92.

30. Abid MR, Yano K, Guo S, Patel VI, Shrikhande G, Spokes KC, et al. Forkhead transcription factors inhibit vascular smooth muscle cell proliferation and neointimal hyperplasia. J Biol Chem 2005;280: 29864–73.

31. Paik JH, Kollipara R, Chu G, Ji H, Xiao Y, Ding Z, et al. FoxOs are lineage-restricted redundant tumor suppressors and regulate endothelial cell homeostasis. Cell 2007;128:309–23.

32. Tomizawa M, Kumar A, Perrot V, Nakae J, Accili D, Rechler MM. Insulin inhibits the activation of transcription by a C-terminal fragment of the forkhead transcription factor FKHR. A mechanism for insulin inhibition of insulin-like growth factor-binding protein-1 transcription. J Biol Chem 2000;275:7289–95.

33. Schmoll D, Walker KS, Alessi DR, Grempler R, Burchell A, Guo S, et al. Regulation of glucose-6-phosphatase gene expression by protein kinase B alpha and the forkhead transcription factor FKHR. Evidence for insulin response unit-dependent and -independent effects of insulin on promoter activity. J Biol Chem 2000;275: 36324–33.

34. Modur V, Nagarajan R, Evers BM, Milbrandt J. FOXO proteins regulate tumor necrosis factor-related apoptosis inducing ligand expression. Implications for PTEN mutation in prostate cancer. J Biol Chem 2002;277:47928–37.

35. Stahl M, Dijkers PF, Kops GJ, Lens SM, Coffer PJ, Burgering BM, et al. The forkhead transcription factor FoxO regulates transcription of p27Kip1 and Bim in response to IL-2. J Immunol 2002;168:5024–31.

36. Cully M, You H, Levine AJ, Mak TW. Beyond PTEN mutations: the PI3K pathway as an integrator of multiple inputs during tumorigenesis. Nat Rev Cancer 2006;6:184–92.

37. Mori N, Kyo S, Sakaguchi J, Mizumoto Y, Ohno S, Maida Y, et al. Concomitant activation of AKT with ERK1/2 occurs independently of PTEN or PIK3CA mutations in endometrial cancer and may be associated with favorable prognosis. Cancer Sci 2007;98:1881–8.

ENABLING TECHNOLOGIES

CDK4 and cyclin D1 allow human myogenic cells to recapture growth property without compromising differentiation potential

K Shiomi[1], T Kiyono[2], K Okamura[3], M Uezumi[1], Y Goto[4], S Yasumoto[5], S Shimizu[6] and N Hashimoto[1]

In vitro culture systems of human myogenic cells contribute greatly to elucidation of the molecular mechanisms underlying terminal myogenic differentiation and symptoms of neuromuscular diseases. However, human myogenic cells have limited ability to proliferate in culture. We have established an improved immortalization protocol for human myogenic cells derived from healthy and diseased muscles; constitutive expression of mutated cyclin-dependent kinase 4, cyclin D1 and telomerase immortalized human myogenic cells. Normal diploid chromosomes were preserved after immortalization. The immortalized human myogenic cells divided as rapidly as primary human myogenic cells during the early passages, and underwent myogenic, osteogenic and adipogenic differentiation under appropriate culture conditions. The immortalized cells contributed to muscle differentiation upon xenotransplantation to immunodeficient mice under conditions of regeneration following muscle injury. We also succeeded in immortalizing cryopreserved human myogenic cells derived from Leigh disease patients following primary culture. Forced expression of the three genes shortened their cell cycle to <30 h, which is similar to the doubling time of primary cultured human myogenic cells during early passages. The immortalization protocol described here allowed human myogenic cells to recapture high proliferation activity without compromising their differentiation potential and normal diploidy.
Gene Therapy (2011) **18**, 857–866; doi:10.1038/gt.2011.44; published online 14 April 2011

INTRODUCTION

Skeletal muscle stem cells of adult muscle are known as muscle satellite cells because they are located adjacent to the plasma membrane of myofibers beneath the basement membrane. The postnatal growth, repair and maintenance of skeletal muscle rely on muscle satellite cells that proliferate and then fuse together to form myotubes. Actually, phenotypic analysis of Pax7-deficient mice strongly suggests that the loss of satellite cells abolishes the regenerative capacity of skeletal muscle.[1,2] The decrease of regenerative capacity of muscle results in muscle dysfunction during both normal aging and progression of muscle-regenerative diseases, such as muscular dystrophies.

Most of the data on the regulation of proliferation and differentiation of muscle satellite cells and their descendant progenitor cells have been obtained from primary cultured chick myogenic cells or mouse myogenic cell lines.[3–5] However, several previous studies strongly suggest that animal myogenic cells do not always use the same pathways to control proliferation and differentiation as human myogenic cells.[6,7] Although animal cell models certainly contribute to understanding the mechanisms of human myogenesis and muscle diseases, the precise and detailed analysis of human myogenic cells is essential for fundamental and therapeutic investigation. Unfortunately, progres-

sively compromised differentiation potential, as well as proliferation potential, is seen in cultured human myogenic cells.[8,9] The limited proliferation capacity and progressive alterations of characteristics of human myogenic cells do not allow us to carry out both qualitative and quantitative analyses with high reproducibility.

Previous attempts have been made to extend the replication capacity of human myogenic cells using viral oncogenes such as simian virus 40 large T antigen and/or the reverse transcriptase component of human telomerase (hTERT).[10] However, no reliable model of immortalized human myogenic cells that exhibit differentiation potential had been established until our previous study.[9] We previously reported that constitutive expression of hTERT and human papillomavirus type 16 gene E7 immortalizes a primary normal human myogenic cell clone designated Hu5. The immortalized human myogenic cell clone Hu5/E18 largely preserves the myogenic phenotype represented by parental Hu5 cells, but their doubling time is approximately 12 h longer than that of primary human myogenic cells during early passages. E7 is an oncogene that inactivates the retinoblastoma protein pRb,[11] and does not transform human myogenic cells. However, we cannot exclude a possibility that E7 also affects other biological functions, including transformation-related pathways.

[1]Department of Regenerative Medicine, National Institute for Longevity Sciences, National Center for Geriatrics and Gerontology, Oobu, Japan; [2]Virology Division, National Cancer Center Research Institute, Tokyo, Japan; [3]Department of Urology, National Center for Geriatrics and Gerontology, Oobu, Japan; [4]Department of Mental Retardation and Birth Defect Research, National Institute of Neuroscience, Nervous, and Muscular Disorders, National Center of Neurology and Psychiatry, Tokyo, Japan; [5]Laboratory of Molecular Cell Biology and Oncology, Kanagawa Cancer Center Research Institute, Yokohama, Japan and [6]Department of Plastic Surgery, Kanagawa Cancer Center Research Institute, Yokohama, Japan
Correspondence: Dr T Kiyono, Virology Division, National Cancer Center Research Institute, 5-1-1 Tsukiji, Chuo-ku, Tokyo 104-0045, Japan.
E-mail: tkiyono@ncc.go.jp
or Dr N Hashimoto, Department of Regenerative Medicine, National Institute for Longevity Sciences, National Center for Geriatrics and Gerontology, 35 Gengo, Morioka, Oobu, Aichi 474-8522, Japan.
E-mail: nao@ncgg.go.jp
Received 10 June 2010; revised 16 September 2010; accepted 28 September 2010; published online 14 April 2011

858

Cellular stress activates a pathway of the cyclin-dependent kinase inhibitor p16^{INK4a}, resulting in premature cell cycle arrest before telomere attrition,[12] probably due to the activation of Rb. The forced expression of wild-type cyclin-dependent kinase 4 (CDK4) enabled hTERT to immortalize primary human myogenic cells, presumably because cdk4 sequesters the increased p16 exclusively when stimulated with dexamethasone and hepatocyte growth factor.[13] In addition, the co-expression of hTERT and Bmi-1, which suppresses p16^{INK4a} expression, failed to immortalize human myogenic cells.[9,14] These results indicate that combining the expression of hTERT and sequestration of p16 ^{INK4a} is insufficient to immortalize human myogenic cells, or that the p16 ^{INK4a} pathway is incompletely suppressed under these conditions.

In the present study, to block the p16^{INK4a}–Rb pathway and enhance cell cycle progression, without the use of oncoprotein E7, expressions of hTERT and both mutant CDK4 (CDK4R24C) and cyclin D1 were induced in human myogenic cells. Combined expression of the three genes efficiently immortalized normal human myogenic cells. The immortalized cells still retained multipotentiality and a doubling time similar to that of primary cultured human myogenic cells. The established normal human myogenic cell clones in the present study are the human equivalents of mouse cell lines such as C2 (ref. 3) and Ric10.[5,15] In addition, we succeeded in immortalization of diseased muscle-derived primary human myogenic cells that showed the prolonged doubling time. The newly established method for immortalization of primary human myogenic cells will open new avenues for mechanistic and therapeutic research on human muscle diseases.

RESULTS

p16 ^{INK4a}–Rb pathway is activated upon growth arrest of primary cultured human myogenic cells

Proliferation capacity of primary cultured human myogenic cells severely declined during serial passages under the present culture condition (Figure 1a). The doubling time of the cells became longer as they were serially succeeded (Supplementary Figure 1). Constant or
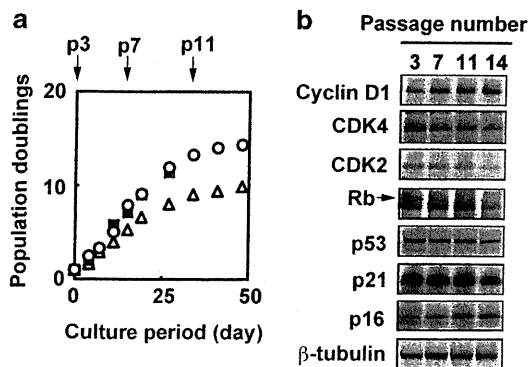

Figure 1 Growth properties of primary cultured human myogenic cells. (a) Life span plots of primary cultured human myogenic cells Hu20 (filled square), Hu23 (triangle) and Hu26 (circle) between passages 3 and 13. Arrows show the timing of passages 3, 7 and 11. Day 0 of culture period represents the day when the cells were plated for passage 3. (b) Expression patterns of growth-related proteins in primary cultured human myogenic cell H23 during serial passages. Fifteen micrograms of total proteins were subjected to immunoblotting analysis with antibodies against proteins shown in the left panels. Similar expression patterns of the proteins were obtained in Hu20 and Hu26. An arrow represents the position of hyperphosphorylated Rb protein.

high level expression of cyclin D1, CDK4, cyclin-dependent kinase inhibitor p21^{cip1} and p53 was observed in primary human myogenic cells even upon growth arrest (Figure 1b). In contrast, the amount of the cell cycle inhibitor p16^{INK4a} increased along with the culture period, whereas the amount of hyperphosphorylated form of Rb declined. The amount of another cell cycle-driving kinase CDK2 decreased following the disappearance of hyperphosphorylated form of Rb. The results indicate that the p16 ^{INK4a}–Rb pathway is activated before growth arrest of primary cultured human myogenic cells, suggesting that their cell cycle arrest is due to the activation of Rb. The disappearance of hyperphosphorylated Rb seems unlikely to depend on the downregulation of either CDK2 or CDK4 that are kinases relevant for phosphorylation of Rb.

E7 promotes nuclear progression in terminally differentiated myotubes

The primary human myogenic progenitor cell clone Hu5 was obtained from a healthy muscle of a non-dystrophic woman.[4] Hu5 cells have limited ability to proliferate but can be immortalized by constitutive expression of both telomerase and the E7 gene from human papillomavirus type 16.[9] E7 inactivates Rb but is also suspected to affect other cellular functions. To determine whether constitutive expression of E7 transforms human myogenic cells, the Hu5-derived myogenic cell clone Hu5/E18 (ref. 9), immortalized by constitutive expression of both hTERT and E7, was transplanted into cardiotoxin-injected TA muscles of immunodeficient NOD/Scid mice (Figures 2a and b). Before transplantation, E18 cells were infected with a lentivirus vector encoding green fluorescent protein Venus (kindly provided by Dr Miyoshi). Transplanted cells were identified by the fluorescence of Venus and antibodies specific for green fluorescent protein. Transplanted E18 cells (2.5×10^6 cells per TA) gave rise to myofibers labeled with green fluorescence. No tumor was formed in the transplanted TA muscles. Soft agar assays also showed that E18 was unable to grow in an anchorage-independent way (Supplementary Figure 2). The results indicate that E18 cells did not show any oncogenic potential either in vivo or in vitro.

In the next experiment, effects of the immortalization on cell cycle exit during terminal muscle differentiation were analyzed in vitro. E18 cells undergo myogenic terminal differentiation under the myogenic differentiation-inducing condition.[9] Primary cultured human myogenic progenitor cells exited the cell cycle and gave rise to terminally differentiated myotubes (Figures 2c–f). In contrast, the nuclei of E18 myotubes synthesized DNA and also contained the proliferation marker protein Ki-67, although neither nuclear nor cellular division was observed in the myotubes (Figures 2g–j). The results suggest that E7 promotes nuclear progression in terminally differentiated myotubes that have lost mitogenic potential. In addition, the doubling time of the Hu5-derived immortalized cells is approximately 35 h,[9] whereas primary cultured human myogenic cells divided at 20–29 h intervals (Supplementary Figure 3). Taken together with the results here, the expression of hTERT and E7 immortalizes human myogenic cells without the loss of their differentiation potential but also affects their cell cycle properties during the terminal myogenic differentiation.

Cell cycle drivers efficiently immortalize primary cultured human myogenic cells

E7 promotes nuclear progression in myotubes, perhaps, because it accelerates the degradation of Rb family proteins including Rb, p130 and p107. To inactivate Rb directly and avoid unusual promotion of nuclear progression in myotubes, Hu5 cells were infected with recombinant lentiviruses encoding hTERT, CDK4R24C and cyclin D1.